

TITLE: REACTION RATES FROM PRESSURE-GAUGE MEASUREMENTS  
IN REACTING EXPLOSIVES

**MASTER**

AUTHOR(S): M. J. GINSBERG, ALLAN B. ANDERSON, AND  
JERRY WACKERLE

SUBMITTED TO: FIRST SYMPOSIUM ON GAUGES AND PIEZORESISTIVE  
MATERIALS, ARCACHON, FRANCE, SEPTEMBER 29-30,  
& OCTOBER 1, 1981

University of California



By acceptance of this article, the publisher recognizes that the U.S. Government retains a non-exclusive, royalty-free license to publish or reproduce the published form of this contribution, or to allow others to do so, for U.S. Government purposes.

The Los Alamos Scientific Laboratory requests that the publisher identify this article as work performed under the auspices of the U.S. Department of Energy.

DISTRIBUTION OF THIS DOCUMENT IS UNLIMITED.



**LOS ALAMOS SCIENTIFIC LABORATORY**

Post Office Box 1663 Los Alamos, New Mexico 87545

An Affirmative Action/Equal Opportunity Employer

## REACTION RATES FROM PRESSURE-GAUGE MEASUREMENTS IN REACTING EXPLOSIVES

by

M. J. Ginsberg, Allan B. Anderson, and Jerry Wackerle

### ABSTRACT

The proper hydrodynamic data and an equation of state are sufficient to describe quantitatively the reaction rates of explosives during the shock-to-detonation transition. Piezoelectric pressure gauges embedded in the reacting explosive have provided these data for the explosives PETN, PBX 9404, TATB, and TNT. Once a pressure-field history has been assembled from individual pressure histories at different depths in the explosive, the conservation equations can be applied in a Lagrangian analysis of the data. The combination of a reactant-product equation of state with this analysis then allows the calculation of the extent of reaction and reaction rate. Successful correlation of the calculated reaction rate values with other thermodynamic variables, such as pressure or temperature, allows formulation of a rate law and the prediction of initiation behavior under circumstances quite different from the experiments that led to the rate law.

The best dynamic piezoelectric pressure gauge for most applications would have a substantial output voltage and present negligible disturbance to the flow. In explosives, however, requirements for survival in the extreme temperature and pressure environment encountered by the gauge dictate compromise. Low electrical resistance ( $\sim 20 \text{ m}\Omega$ ) helps to minimize shunt conductivity failures, but this drastically reduces output and demands that much attention be given to reducing noise. Although relatively thick insulation perturbs the flow to some extent, survivability requirements dictate its use. Pressure measurements in reactive flow can now be made routinely with gauges that successfully produce data leading to a description of the flow and a powerful predictive capability.

ar shock gas gun experiments with embedded pressure gauges are fine the pressure histories at a number of Lagrangian positions (mass points that move with the flow) in the initiating explosive. Lagrangian analysis is done to obtain, by interpolation, the pressure histories, and to integrate the conservation relations for the density-, and energy-field histories throughout the distance-time re-

## I. INTRODUCTION

A global reaction progress variable is defined and incorporated into the continuity-energy equation of state, and the decomposition rate calculated throughout the reactive flow.

causes an exothermic detonation. I wave velocity, quantities, such as have been inferred from measurements by yielding results in the zone of reaction of submillimeter tails of the pressure the kinetics of use of pressure

If the in space-time region longer time than position in the we might follow before the trans

pressure or particle velocity of sufficient amplitude propagating in a chemical explosive opportunity to start a thermic reaction (or shock-induced decomposition) that can lead to when studying important variables associated with steady detonation, such as the detonation pressure can be measured routinely and accurately(1). Other important variables such as the detonation pressure--typically 25 to 40 GPa--have usually been measured from indirect measurements(2), although direct detonation pressure measurements have recently been performed with embedded piezoresistive gauges(3,4) which give the time history in substantial agreement with calculations. However, because the shock action behind the shock front in a detonating explosive is normally of the order of millimeter thickness, such measurements do not provide time-resolved detonation pressure history in the reaction zone. Therefore, determination of the time-resolved value of shock-induced decomposition in a steady detonation through the use of embedded gauges is not possible with existing techniques.

Embedded Lagrangian analysis in which the shock-induced decomposition takes place over a few millimeters in a detonation. Typically, although there might be full decomposition of reactive submillimeter reaction zone of a detonation in less than 0.1  $\mu$ s, the time and analytical evolution of pressure waves over a span of about 10 mm and 2  $\mu$ s belong to the Lagrangian piezoresistive gauges.

Our goal is to study the kinetics of shock-induced decomposition that is denied by the current procedure.

(1) Planning to describe initiation phenomena does, however, raise difficulties used to determine the time history of detonation phenomena. Initiation is a nonsteady process (that is, at the time of initiation there is no relatively simple and accurate theoretical background(5) to describe the process.)

(2) A Lagrangian analysis and distance required for the explosive to transit from initial velocity to detonation, and some measure of the intermediate shock velocity history of the explosive, a detailed picture of the process (pressure, volume, and expansion of the explosive as a function of distance and time in the reacting material) has

(3) A Lagrangian analysis is not possible until the advent of gauges and techniques that yield time-resolved histories of the hydrodynamic variables associated with the decomposition.

Lagrangian pressure and particle velocity gauges and the associated analysis techniques do yield these time-resolved measurements and offer the possibility of obtaining a description of the global decomposition kinetics of explosives. In this paper we will concentrate on the experimen-

(4) Position-independent correlations of the rate with the other thermodynamic variables are sought, and when found, formulated as empirical rate laws for the decomposition kinetics.

(5) These rate laws are tested for general validity with numerical hydrodynamic simulations of shock-initiation experiments that are quite different from those generating the rates.

Pressure gauge measurements in reacting pentaerythritol tetranitrate (PETN) made by Wackerle, et al.(8), were accompanied by an analysis through step 3 of the preceding paragraph, and Soviet researchers studying trinitrotoluene (TNT)(9, 10) proceeded one step further. Analytical methodologies are discussed in these references, and in Ref. 11. The complete procedure was successfully carried out at our laboratory on PEX 9404(12), a plastic-bonded explosive, and the insensitive high explosive trinitrotrinitrobenzene (TATB)(13). These two studies led to the formulation of the shock-strength dependent rate law DAGMAR\*, which will be described in more detail in Section V. Other investigators have performed embedded gauge measurements in reacting explosives(14), but did not obtain reaction rate laws based on their data.

## II. EXPERIMENTS

As an illustration of our experimental techniques, we describe recent work we have done on TATB(13). TATB cylinders were pressed from a powder having a modal particle size of approximately 20  $\mu\text{m}$  and then machined into disks. Fabrication conditions were carefully controlled and repeated. The density of the specimens was  $1.80 \pm 0.01 \text{ g/cm}^3$ . Radiographic examination of the disks showed no local density discontinuities large enough to affect the experiments.

Targets for gas gun experiments (see Fig. 1) were fabricated from one grooved disk of a chosen thickness, and one flat disk. A single, low-resistance, four-terminal Manganin gauge was embedded in the grooved disk, and the other disk cemented to the first. The gauges were photoetched from 0.050-mm-thick annealed foil and thermally bonded between two 0.25-mm sheets of FEP Teflon, producing a package slightly over 0.5-mm thick. Typical electrical resistance of the active element of the gauge was 20  $\text{m}\Omega$ . A current of approximately 60 A was provided to the gauge by two power supplies of the type described by Vantine, et al.(4), whose gauge calibration(15) (without hysteresis correction) was used to obtain pressure histories from the gauge records.

The annealed copper flyers used in the sustained shock experiments were 6.35-mm thick (Fig. 2). Those used in the short-shock experiments were 1-mm thick and backed by polymethyl methacrylate (PMMA). The average projectile velocity of 1.17  $\text{mm}/\mu\text{s}$  provided a planar shock of 7.6 GPa amplitude, which leads to detonation in approximately 10 mm in the sustained shock case.

Figure 3 shows measured pressure histories (as solid lines) in TATB obtained under the conditions described above. The dotted lines are calculated values. Calculations will be discussed in a later section. The gauge locations were at 0, 2.3, 3.7, 5.3, 6.7, and 7.7 mm.

---

\*Direct Analysis Generated Modified Arrhenius Rate. Although we no longer use direct analysis (a less refined method of Lagrangian analysis) we have retained the acronym.

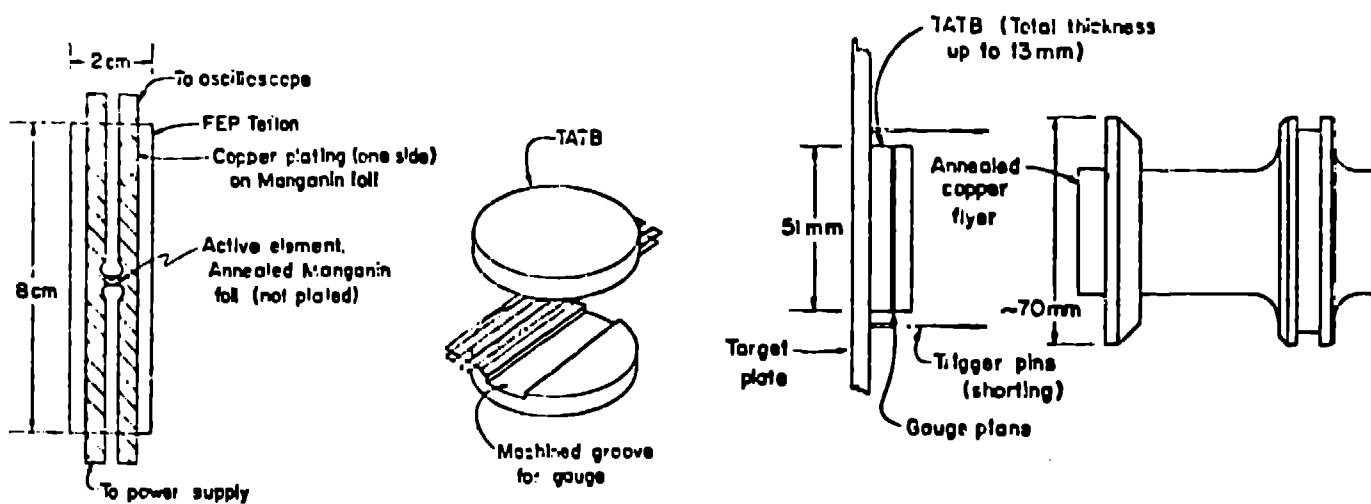


Fig. 1 Low-resistance Manganin gauge and target assembly

Fig. 2 Target and projectile for sustained-shock gas-gun experiments.

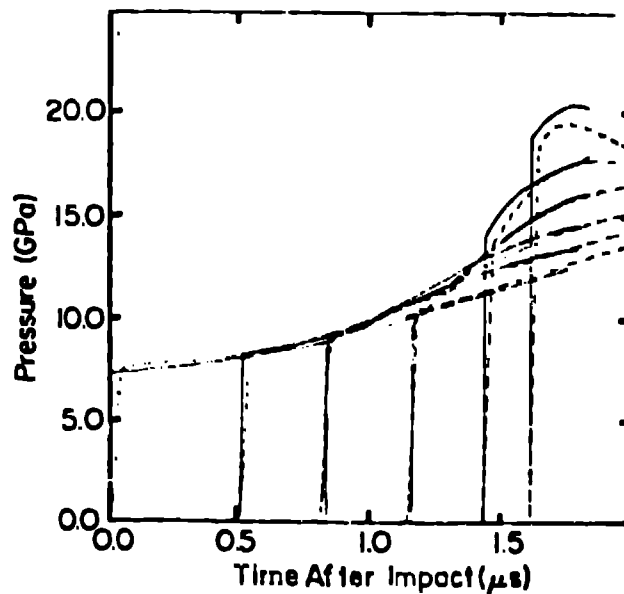


Fig. 3 Observed (solid lines) and calculated pressure histories.

### III. PIEZORESISTIVE GAUGES IN REACTING EXPLOSIVES

The material insulating a piezoresistive gauge in a reacting explosive typically encounters pressures of 10 to 30 GPa and shock temperatures up to 2000°K during its 1- to 3- $\mu$ s lifetime. The explosive decomposition products are hot and electrically conductive, posing the threat of shorting the powering current from the gauge if the insulation fails. Shunt conduction arising from shock-induced conductivity in the insulator itself is also a possibility.

In general, the best dynamic pressure gauge for any given application would produce a substantial output voltage in the pressure regime of interest, and present minimum disturbance to the flow. Minimizing disturbance to the flow consists of minimizing gauge thickness and matching the impedance of the package to the compressed, unreacted explosive as closely as possible. Matching shock impedance and minimizing thickness also improves the time resolution of the gauge. This is most important in the region near the shock front, where pressure changes take place rapidly, and pressure equilibration of the gauge through ringing can mask details of the recorded history. Unfortunately, the extreme conditions encountered by the gauge in a reacting explosive require that we make compromises in insulator thickness and gauge resistance (thereby lowering signal level) in order to insure gauge survival for the desired duration.

The most important problem to be solved is that of shunt conductivity. Depending on the particular gauge design and insulator materials, current can be shunted because of a conducting path between the gauge and the reacting explosive, or because of pressure- or temperature-induced conductivity in the insulator itself, or both. Pressure gauge measurements were made in our laboratory on PETN and PBX 9404 using commercially available 50 $\Omega$  Manganin gauges(8,12). It was concluded that in some instances, conductivity effects caused premature failure of these gauges, which were insulated with a thin layer of Kapton polymer. Kapton has been shown to undergo a considerable increase in conductivity during the passage of a stress wave of the amplitude seen in PETN and PBX 9404 during initiation(16).

We briefly investigated the effect of the reacting explosive environment on Kapton-and-epoxy encapsulated grid gauges (nominally 50 $\Omega$ ). One normal Kapton-backed 50 $\Omega$  grid, and one grid that was made into an open circuit by carefully trimming out the connecting metal between the longer elements, were encapsulated between two 0.050-mm sheets of Kapton glued with epoxy adhesive. A 50 $\Omega$  resistor was wired in parallel with the open grid. The package was embedded behind 4.5 mm of PBX 9404 and the explosive was subjected to an input shock of 2.9 GPa produced by planar projectile impact in a gas gun. The results are shown schematically in Fig. 4. The lead shock reaches the gauge, and is followed by the reactive wave overtaking from the rear. At shock arrival, the 50 $\Omega$  gauge shows a jump to the shock pressure level in the material at that point (point A) and the conductivity probe shows a small decrease in resistance that remains constant until the pressure reaches an apparent maximum of approximately 10 GPa (point B). Here, the conductivity probe shows another small increase, corresponding to an apparent pressure decrease, as shown by the pressure gauge, and then the probe shows what is essentially a runaway conductivity increase, corresponding to a shock-induced conductivity failure of the pressure gauge (point C). The pressure record in this case is not reliable beyond point C. Epoxies and other adhesives as well as other complex polymers have also been shown to undergo increases in conductivity during dynamic compression(16). However, it is interesting to note that Burrows, et al.(3), performed detonation-pressure measurements with Manganin gauges encapsulated in a Teflon package glued together with epoxy. Surprisingly, no

induced conductivity was evident. Champion(17) measured the change in conductivity of shock-compressed Teflon and polyethylene and found a much reduced effect, making these materials look attractive for gauge insulation.

Weingart, et al.(18), performed a number of experiments designed to ascertain whether failure by conductivity occurs inside the gauge package through the reactive explosive. They bonded low-resistance (20-m $\Omega$ ) four-terminal Manganin gauges in PTFE Teflon without an adhesive, but with FEP Teflon in contact with the gauge. The total insulation thickness was varied from 0.13 to 0.50 mm. Their thin gauge packages in reacting PBX 9404 showed clear evidence of early failure, which was attributed to conduction through the reactive explosive. Our work on similar gauges supports this, as is shown in Fig. 5. This figure shows time-to-failure vs gauge depth for different insulation thickness for gauges placed at different depths in reacting TATB. The experimental configuration was seen in Figs. 1 and 2, and Fig. 6 shows a typical gauge record with the onset of conductivity taking place at point A. The thicker insulation clearly allows longer recording time, and suggests that conductivity does take place between gauge and reacting explosive rather than in the package itself. It can also be seen that, within the limits of gauge resistance (20 to 80 m $\Omega$ ) considered, the gauge resistance is a secondary effect.

The choice of a low resistance (20-40 m $\Omega$ ) active element was made primarily to avoid shunt conductivity in the gauge package itself. The resistance of the conducting path in the Teflon insulator for typical gauge dimensions is approximately 20 $\Omega$ , based on Champion's data(17). Gauges of lower resistance might also be less likely to fail through contact with the reacting explosive. However, in the narrow range of resistance we have studied (20 to 80 m $\Omega$ ) the data in Fig. 5 provide no conclusive evidence. With a powering current of 60A, the output of a 20 m $\Omega$  gauge is approximately 25 mV/GPa, producing peak signal levels in a typical experiment of 200 mV. At this level we rarely see persistent electrical noise. Although noise spikes of greater than 10 mV amplitude do occasionally occur, the system usually recovers within 0.1  $\mu$ s, and the record is not severely affected.

With 0.25 mm of FEP Teflon insulation on each side of the gauge, recording duration of 2 to 2.5  $\mu$ s is routinely achieved, even at deep stations where the measured pressure is over 20 GPa. Also, the Teflon is a reasonable impedance match to the reacting explosive, and allows adequate response to the shock and following wave. As can be seen from the record shown in Fig. 6, there is no resolvable overshoot at the top of the lead shock and a quick recovery, allowing the rest of the wave to be faithfully recorded.

Although it is inevitable that the placement of a 0.5-mm thick gauge package in the reacting explosive must disturb the flow, the experimental evidence of Weingart, et al.(18), suggests that the disturbance is not as great as might be expected. However, this is insufficient comfort, because just as we know that increasing gauge thickness will ultimately affect the flow to an unacceptable extent, decreasing that dimension must produce less disturbance. The answer to this problem probably depends on the development of an improved insulator that, while retaining the shock-impedance matching properties of Teflon, represents an improvement in its ability to resist the mechanism that leads to shunt conductivity. Until such a material is found, heat-bonded Teflon will continue to be our choice in this application. It is also possible, however, that our requirements for duration might be met by the times-to-failure shown in Fig. 5 for gauges insulated by only 0.13 mm of Teflon on each side. In fact, the analysis of TATB data discussed in the following sections required gauge lifetimes only as long as those obtained with 0.13-mm insulation.

#### IV. LAGRANGIAN ANALYSIS

The Lagrangian analysis of gauge data is effected by the successive integration of the fluid-dynamic conservation relations for momentum, mass and energy. In terms of the initial (Lagrangian) position coordinate,  $h$ , and time,  $t$ , these relations are:

$$\partial u / \partial t = -v_0 \partial p / \partial h, \quad \partial v / \partial t = v_0 \partial u / \partial h,$$

$$\text{and } \partial e / \partial t = -p \partial v / \partial t = -p v_0 \partial u / \partial h,$$

where  $p$ ,  $u$ ,  $v$ , and  $e$  are the pressure, particle velocity, specific volume and specific internal energy, respectively, and the sub-0 denotes the initial, unshocked, value.

For our TATB study, we adopted a "pathline" method similar to that developed by Seaman(19), who extended the work of Grady(20). In this approach, we transform the real time coordinate  $t$ , to a pathline coordinate  $t(h)$  and use directional derivatives to replace the gradients  $\partial p / \partial h$  and  $\partial u / \partial h$ . In integral form, the transformed equations become

$$u(h,t) = u_1(h) - v_0 \int_{t_1(h)}^{t(h)} \left[ \frac{dp}{dh} - \frac{\partial p(h,t')}{\partial t'} \frac{dt'(h)}{dh} \right] dt',$$

$$v(h,t) = v_1(h) + v_0 \int_{t_1(h)}^{t(h)} \left[ \frac{du}{dh} - \frac{\partial u(h,t')}{\partial t'} \frac{dt'(h)}{dh} \right] dt',$$

$$e(h,t) = e_1(h) - v_0 \int_{t_1(h)}^{t(h)} p(h,t') \left[ \frac{dv}{dh} - \frac{\partial v(h,t')}{\partial t'} \frac{dt'(h)}{dh} \right] dt'.$$

Here the total derivatives are along the pathline and the partial derivatives are at fixed  $t$  or  $h$ , and the sub-1 indicates values along the first path. Although the transformation might be suspected of introducing greater error in the analysis, this is not the case. No error is introduced by the term  $dt/dh$ , because we choose  $t(h)$  arbitrarily, and  $\partial p / \partial t$  is evaluated through dense data (unlike  $\partial p / \partial h$ ). In addition, paths can be chosen to minimize the variation in pressure along the path so that the evaluation of  $dp/dh$  is generally superior to that of  $\partial p / \partial h$ .

In our use of the pathline method, we choose the shock locus as the first path, and construct the other paths so that data from all the gauges are used throughout the calculation (see Fig. 7). State parameters along the shock path are defined by the Hugoniot relations for conservation of momentum, mass and energy:

$$v_0 P_1 = u_1 U_1, \quad v_1 / v_0 = 1 - (u_1 / U_1), \quad \text{and } e_1 - e_0 = (P_1 / 2) (v_0 - v_1),$$



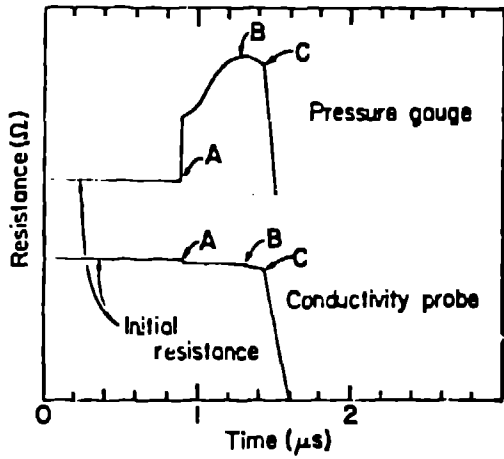


Fig. 4 Evidence of shunt conductivity failure in a  $50\Omega$  gauge. Complete failure begins at point C.

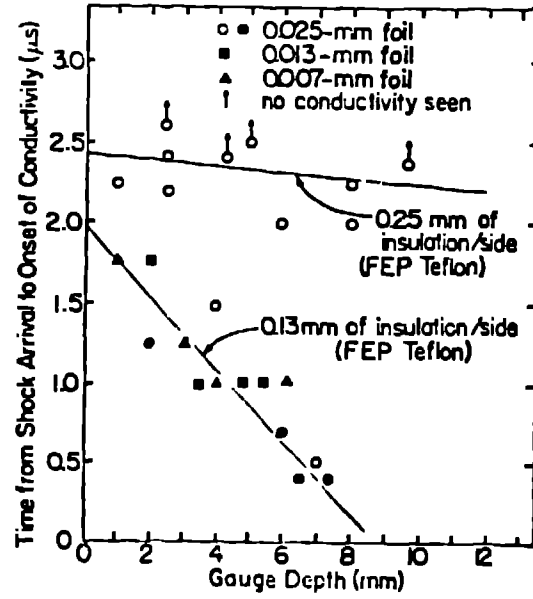


Fig. 5 A comparison of times-to-failure for Manganin foil gauges in reacting TATB insulated with 0.25mm and 0.13 mm of FEP Teflon on each side of the gauge.

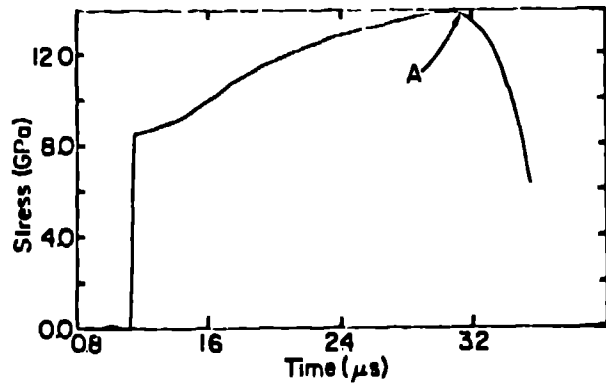


Fig. 6 Pressure gauge record obtained in reacting TATB at a depth of 2.3 mm. Shunt conductivity begins at point A.

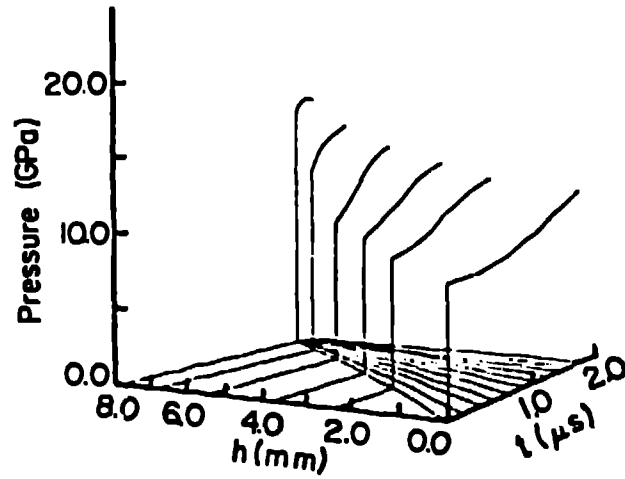


Fig. 7 Pressure histories and sample pathlines.

where  $U_1$  is the shock velocity. We complete this description by specifying the shock Hugoniot for the explosive in the common form  $U_1 = C + Su_1$ , with the constants  $C$  and  $S$  evaluated from auxiliary (usually explosive wedge) experiments.

The fitting of real (estimated to be accurate within 5%) data is something of an exercise in curve fitting. The calculated specific volumes and energies essentially depend on the curvature of  $p(h)$ . We have found that fitting  $p(h)$  with cubic splines, which minimize the total curvature, gives good results relatively free of nonphysical oscillations in  $v$  and  $e$ .

## V. EQUATION OF STATE AND RATE CALCULATION

The Lagrangian analysis provides a history of pressure, specific volume and energy at the gauge locations. Relating a reaction progress variable to these three state variables through an equation of state allows the calculation of decomposition rates. The rates are, of course, valid only for the particular equation-of-state relationship chosen.

Equations of state are commonly formulated with the assumption that the decomposing explosive is a mixture of unreacted solid and fully reacted, primarily gaseous products. The relationship is thus a construct of the  $p$ - $v$ - $e$  equations for the two components, a reaction progress variable equal to the mass fraction of one of the components (we use that of the products, denoting  $\lambda=0$  as unreacted and  $\lambda=1$  as fully reacted), and a "mix rule" that, explicitly or implicitly, divides the specific internal energy between the two components.

Presently, we use the HOM equation of state(21). The component state relationships are both Mie-Grüneisen forms, that is:

$$p(v,e) = p_r(v) + (\Gamma/v) (e - e_r)$$

where  $\Gamma = v(\partial p / \partial e)$  is the Grüneisen ratio and the sub- $r$  denotes values along a reference curve. For the solid, this reference is taken as the shock Hugoniot, calibrated to measurements as described above, and the good approximation of  $(\Gamma/v) = \text{constant}$  is assumed. The reference curve for the products is taken as the isentrope through the Chapman-Jouget (CJ) detonation state expressed in the Becker-Kistiakowsky-Wilson form(22). Although this is a calculated relationship, it is well calibrated to shock-wave data on product species and to detonation velocities of the well-studied explosives. The mix rule is defined with the assumptions of ideal mixing of the specific volume and energy and of equilibrium of pressure and temperature between the two components. Temperatures along reference curves for the two components are defined by the equation-of-state assumptions already stated, and are calculated at points off these reference curves with the additional assumption of constant specific heat.

## VI. RATE CORRELATION

The analysis at this point provides numerical values of the pressure, density, internal energy, temperature, degree of decomposition and reaction rate at each gauge location. If correlations of the rate values to combinations of other state variables can be found that hold throughout the reactive flow, they can serve as empirical rate laws for the explosive. The calculated "data" can also serve to test various proposed theoretical or empirical rate forms.

With both PBX 9404 and TATB, we have obtained the best results by examining the rate dependence on temperature in a simple Arrhenius form. Assuming first-order depletion, the calculated rates for TATB are shown by the solid curves in Fig. 8. The results are similar to those obtained with PBX 9404, and suggest the same form for the rate. The parallel curves suggest the use of a single activation energy or temperature for the rate, but some modification of the pre-exponential factor is necessary. Because both this factor and the shock strength are monotonically increasing for the deeper gauge locations, it seems appropriate to introduce some measure of shock strength into the rate. Using the shock pressure,  $p_s$ , as this measure, we examined the correlation:

$$\dot{\lambda}/(1-\lambda) = Z_0 p_s^n e^{-T^*/T}$$

We found that this DAGMAR form agrees reasonably well with the calculated rates. A least squares analysis, minimizing deviations in the "experimental" rate-time space of Fig. 8, gives the set of constants:  $Z_0 = 0.0158$ ,  $n = 2.61$  and  $T^* = 1861K$ , where  $\mu s^{-1}$  rates and GPa pressure units are used. The correlation to the calculated rates with these constants is indicated by the dashed lines in Figs. 8 and 9.

The correlation is essentially the same as that first obtained with PBX 9404, where analysis of both sustained- and short-shock initiation configurations with a 2.9-GPa input shock strength (but run distance to detonation similar to the TATB experiments) gave  $Z_0 = 0.17$ ,  $n = 2$  and  $T^* = 1200 K$  as constants. The DAGMAR form for PBX 9404 also included a modest induction time factor, but this may have resulted from a constraint imposed on the direct analysis performed for that explosive.

## VII. DISCUSSION AND CONCLUSIONS

A principal motive for determining empirical rate forms is to provide information for the modeling of initiation and detonation phenomena with numerical hydrodynamic calculations. The successful simulations of experiments involving shock configurations and state conditions quite different from those used in obtaining the correlation allow more confidence in the generality of the derived rate. Such modeling is done with numerical hydrocodes that operate on the fluid dynamic conservation relations in finite difference form, advancing the calculation in small time increments. An assumed rate law is used to update the reaction coordinate, and the  $p(v,e,\lambda)$  relation is used to calculate the pressure for the next time cycle. In our simulations, we use the PAD 1D hydrocode developed by Fickett(22) with our addition of the HOM equation of state.

A first requirement of our rate law is that it gives simulations of the pressure data used to generate it. PAD calculations of the gauge-pressure histories were shown as dashed lines in Fig. 3. The good agreement signifies only that we made no serious error in the analysis.

A more demanding test is simulation of gauge data with short-shock inputs. For TATB, we performed the same experiments described previously, except that the thick flyer (Fig. 2) was replaced with one that was 1-mm thick. A series of experiments gave the gauge records shown as solid lines in Fig. 10. Computer simulations with the calibrated DAGMAR form gave the dashed curves, in reasonably good agreement with observation.

Another test of the rate is afforded by data from explosive wedge experiments. In this most common initiation experiment, a planar shock is introduced into a wedge-shaped specimen, and the shock front progress is monitored with a streak camera as it builds up to detonation. The data are commonly displayed in "Pop-plot" form, relating the distance to detonation  $D$  to input shock pressure  $p_i$  as  $D = Ap_i^B$ , with  $A$  and  $B$  constants. Our experiments on 1.8-g/cm<sup>3</sup> TATB were done with high-explosive driving systems, with shock strengths substantially higher and run distances much shorter than those of the embedded-gauge experiments. The streak-camera records typically displayed an initial constant wave velocity region, a break to an intermediate accelerating region, and a second break continuing to the onset of detonation. Both breaks fit the Pop-plot form, as shown by the open symbols in Fig. 11. Numerical hydrodynamic calculations of these build-up features, shown as crosses in Fig. 11, are in excellent agreement with observation.

In addition to the examples given above, DAGMAR forms have provided computer simulations of nearly all of the existing planar shock initiation data base on PBX 9404 and 1.8-g/cm<sup>3</sup> TATB. The data base for PBX 9404 is substantial, including all of the experiments described above and numerous short-shock sensitivity tests and experiments in which plates are accelerated by partially reacted explosive. There are also high-pressure short-shock sensitivity test results for TATB(23), which we have also calculated successfully. Reaction rate formulations obtained from embedded gauge data coupled with Lagrange analysis and an assumed equation of state yield useful and important information about the shock-induced decomposition of explosives.

We believe that the Teflon-armored low-resistance Manganin gauge yields pressure-field histories in reacting explosives of sufficient quality to be used as the data for Lagrangian analysis and subsequent reaction rate derivation.

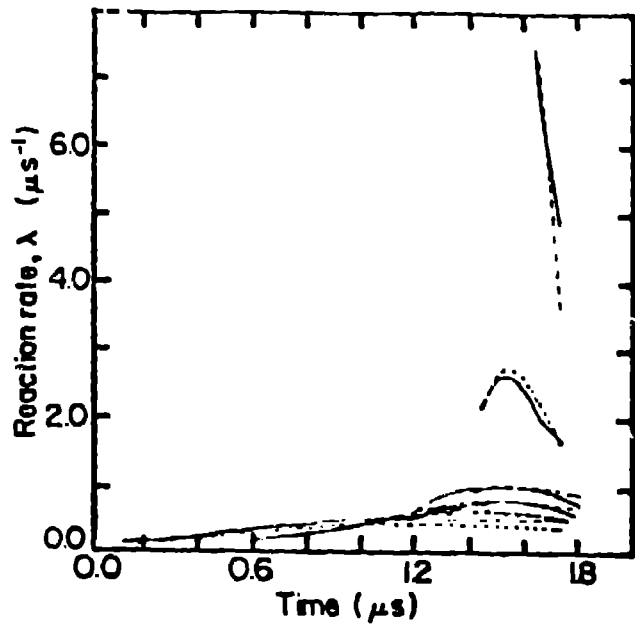


Fig. 8 Calculated reaction-rate histories at gauge locations.

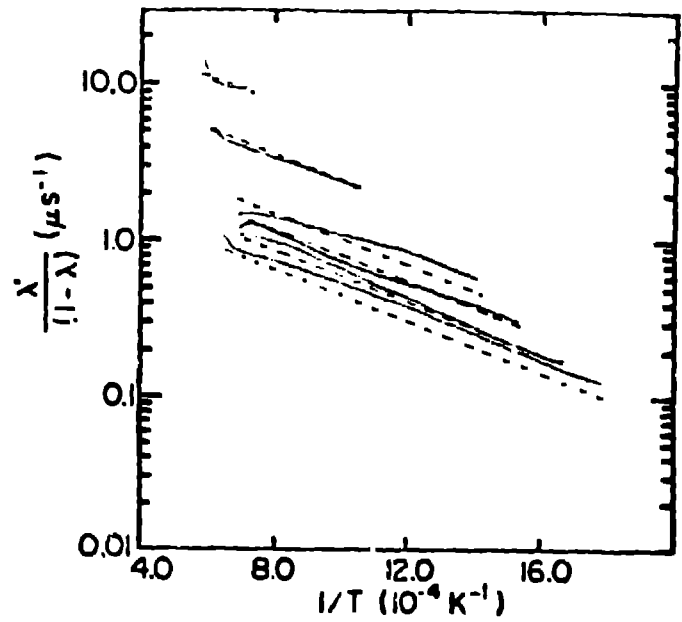


Fig. 9 Arrhenius representation of calculated reaction rates.

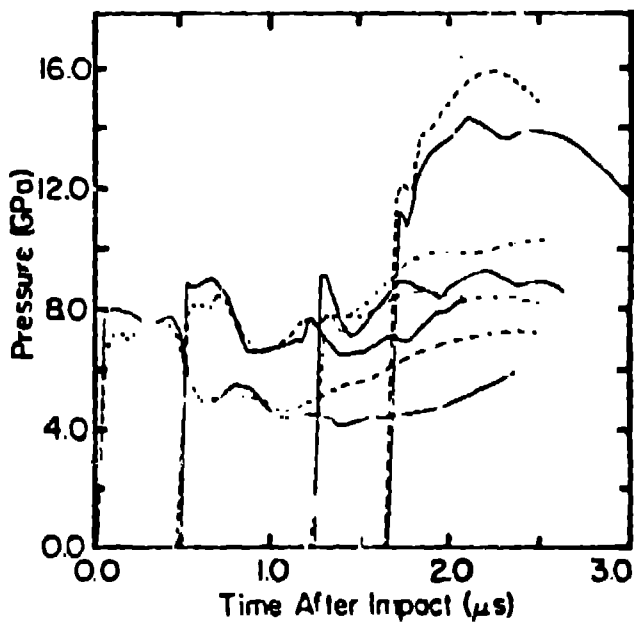


Fig. 10 Observed and calculated pressure histories with a short-shock input.

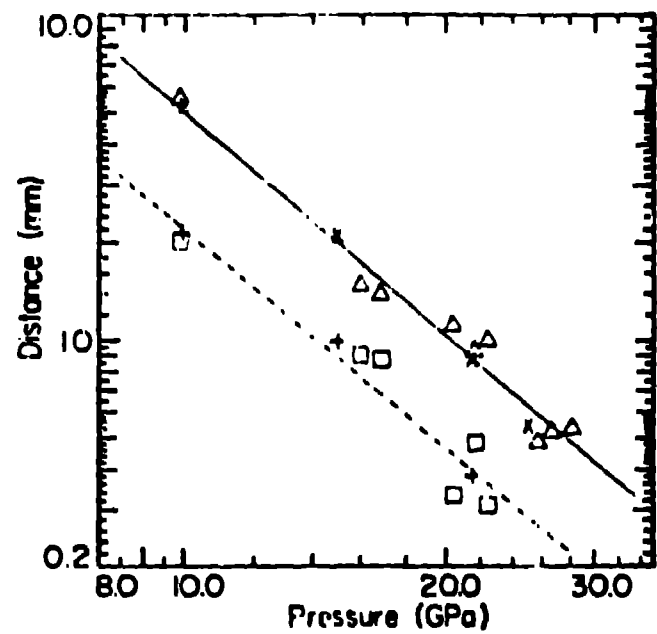


Fig. 11 Pop-plot representation of explosive-wedge data.

## REFERENCES

1. A. W. Campbell and Ray Engelke, "The Diameter Effect in High-Density Heterogeneous Explosives," Proc. Sixth Symp. (International) on Detonation, Office of Naval Research report ACR-221, 1976, p. 642.
2. W. C. Davis and D. Venable, "Pressure Measurements for Composition B-3," Proc. Fifth Symp. (International) on Detonation, Office of Naval Research report ACR-184, 1970, p. 13.
3. K. Furrows, D. K. Chilvers, R. Fyton, B. D. Lambourn, and A. A. Wallace, "Determination of Detonation Pressure Using a Manganin Wire Technique," Proc. Sixth Symp. (International) on Detonation, Office of Naval Research report ACR-221, 1976, p. 625.
4. H. Vantine, J. Chan, L. Erickson, J. Janzen, and R. Weingart, "Precision Stress Measurements in Severe Shock Wave Environments with Low-Impedance Manganin Gauges," Rev. Sci. Instrum., 51, 116, 1980.
5. W. Fickett and W. C. Davis, Detonation, (University of California Press, Berkeley, 1979).
6. J. M. Majewicz and S. J. Jacobs, "Initiation to Detonation of High Explosives by Shocks," Bull. Am. Phys. Soc., 5, 293, 1958.
7. A. W. Campbell, W. C. Davis, J. G. Ramsay, and J. R. Travis, "Shock Initiation of Solid Explosives," Physics of Fluids, 4, 511, 1961.
8. Jerry Wackerle, J. O. Johnson, and P. M. Halleck, Proc. Sixth Symp. (International) on Detonation, Office of Naval Research report ACR-221, 1976, p. 20.
9. G. I. Kanel, "Kinetics of the Decomposition of Cast TNT in Shock Waves," Fizika Goreniya i Vzryva, 14, 113, 1978.
10. G. I. Kanel and A. N. Dremin, "Decomposition of Cast Trotyl in Shock Waves," Fizika Goreniya i Vzryva, 13, 85, 1977.
11. M. Cowperthwaite, "Determination of Energy Release Rate with the Hydrodynamic Properties of Detonation Waves," Fourteenth Symposium (International) on Combustion, (The Combustion Institute, Pittsburgh, 1973), p. 1259.
12. Jerry Wackerle, R. L. Fable, M. J. Ginsberg, and A. B. Anderson, "A Shock Initiation Study of PBX 9404," Proceedings of the Symposium on High Dynamic Pressures, Paris, France, 1978, p. 127.
13. Allan B. Anderson, M. J. Ginsberg, W. L. Seitz, and Jerry Wackerle, "Shock Initiation of Forous TATB," Proc. Seventh Symp. (International) on Detonation, Preprints, 1981, p. 584.
14. L. Green, E. Nidick, E. Lee, and C. Tarver, "Reactions in PBX 9404 from Low-Amplitude Shock Waves," Proceedings of the Symposium on High Dynamic Pressures, Paris, France, 1978, p. 115.

15. H. C. Van der Broek, J. M. F. de Groot, and J. P. de Groot, "Hydrodynamic In-Corrected Galilean Transformations Under Shock Conditions," *J. Appl. Phys.* 51, No. 4, p. 1917, 1980.
16. R. A. Johnson, "Electrical Switching of Shock Loaded Polymeric Films," *Full. Am. Phys. Soc.*, 24, 711, 1979.
17. A. R. Champion, "Effect of Shock Compression on Electrical Resistivity of Three Polymers," *J. Appl. Phys.*, 43, 2216, 1972.
18. R. Weingart, P. Parlett, S. Cochran, L. Erickson, J. Chan, and J. Janzen, "Magnain Stress Gauges in Reacting High Explosive Environment," *Proceedings of the Symposium on High Dynamic Pressures*, Paris, France, 1978, p. 451.
19. Lynn Seaman, "Lagrangian Analysis for Multiple Stress or Velocity Gages in Attenuating Waves," *J. Appl. Phys.* 45, 4303, 1974.
20. P. E. Crady, "Experimental Analysis of Spherical Wave Propagation," *J. Geophys. Res.*, 78, 1299, 1973.
21. Charles L. Fuder, Numerical Modeling of Detonation, (University of California Press, Berkeley, 1979).
22. W. P. Pratt, "PAD, A One-Dimensional Hydrocode," Los Alamos Scientific Laboratory report LA-5910-MS, 1975.
23. G. Knodel, J. Humphrey, R. Weingart, R. S. Lee, and P. Kramer, "Shock Initiation of TATB Formulations," *Proc. Seventh Symp. (International) on Detonation*, Preprints, 1981, p. 632.